

General Participative Media Single Image Restoration

Joel D.O. Gaya *, Felipe Codevilla *, Amanda C. Duarte and Silvia Botelho
Universidade Federal do Rio Grande (FURG)
Rio Grande - Brazil

felipe.codevilla@furg.br

Abstract

This paper describes a method to restore degraded images captured in general participative media — fog, turbid water, sand storm, etc. To obtain generality, we, first, propose a novel interpretation of the participative media image formation by considering the color variation of the media. Second, we introduce that joining different image priors is an effective alternative for image restoration. The proposed method contains a Composite Prior supported by statistics collected on both haze-free and degraded participative environment images. The key of the method is joining two complementary measures — local contrast and color. The results presented for a variety of underwater and haze images demonstrate the power of the method. Moreover, we showed the potential of our method using a special dataset for which a reference haze-free image is available for comparison.

1. Introduction

A *participative media* is defined as any kind of media where the particles in suspension in the media affect the image formation, *e.g.* underwater media, fog, sand storm, etc. (See Fig. 3 for samples). Images taken in these types of environments are degraded by these particles. This happens since light is *scattered* and *absorbed*, culminating into scene information loss. Also, the particles from outside the scene scatter over the image producing a characteristic veil which reduces the image contrast.

Most of the image restoration methods attempt to recover degraded images relying on a physical model of the image formation. The used physical model describes a linear superposition between the signal and the veil. To recover the degraded images, the methods have to estimate (i) the color and radiance properties of the veil, also called *veiling light*, and (ii) the amount of veil on each image patch, *i.e.* the *transmission*. This is an oddly-posed problem, since there

is plenty of information ambiguity in a single image patch. Thus, many methods in the literature use multiple images, polarization [22] or special hardware [12]. To estimate (i) and (ii) from a single image we need to define some image priors which contain information that indicates the transmission and the veiling light.

Most of the single image restoration algorithms are made to specific kinds of participative media, and sometimes lead to impressive results, *e.g.* He *et al.* [13] and Fattal [9] for images with haze around them, or Ancuti *et al.* for underwater images [1]. However, a simple change in the lighting, or sometimes in the structure of the imaged scene, can make a specific method fail. We believe that a more general indication of turbidity is needed in order for an image restoration method to be more robust to environment changes.

In this context, we propose an automatic single image restoration method designed to work in general participative media. Generality is obtained through the contribution toward a new physical model simplification that assumes that the veiling light is the same as the illumination of the objects, *i.e.* the *ambient light*. We are then able to estimate the veiling light using robust color constancy algorithms [10].

Further, in order to obtain robustness we propose an image prior integration scheme. We integrate two different, yet complementary, transmission indicators. The first prior, the *Veil Difference Prior*, assumes that the difference between the channel with the maximum difference to the ambient light in a haze-free image is equal to one. We assume that the visibility (transmission) is proportional to the difference to the ambient light. The second prior, the *Contrast Prior*, assumes that non-turbid images have high contrasts in certain patches. Thus, we infer that the transmission is proportional to a contrast measure. Finally, the priors are joined by assuming that a higher indication of transmission is less likely to be wrong.

With the proposed transmission indication, we are able to successfully restore both haze and underwater images without any parameter change. We compare the results qualitatively, by image examination, and also quantitatively, by a direct comparison with a ground truth.

*Both authors had equal contribution on the design of this paper.

2. Image Formation Model

When the light propagates in a participative environment it is scattered and absorbed by the suspended particles. The *scattering* and *absorption* cause effects on the image formation. The image *signal*, *i.e.* the imaged scene, suffers from *attenuation*, such that just part of the information reaches the camera. Further, the scattering degrades the image formation. *Forward scattering* happens when the light rays coming from the scene are scattered in small angles creating a blurry effect on the image. This effect, however, has a small contribution to the total image degradation and is frequently neglected [22]. Another effect, the *backscattering*, happens when the information from other sources scatters over the camera plane creating a characteristic veil on the image which reduces the contrast and further attenuates the signal information. We define an image captured in a participative environment, for each color channel $\lambda \in \{r, g, b\}$, as

$$I_\lambda(x) = E_{d_\lambda}(x) + E_{bs_\lambda}(x), \quad (1)$$

where $E_{d_\lambda}(x)$ is the direct component (signal) and $E_{bs_\lambda}(x)$ is the backscattering component. The rest of this section explains each of the components of Eq. (1).

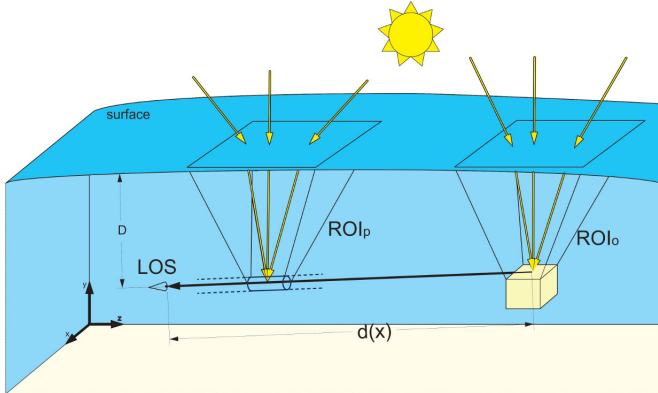


Figure 1: The image formation model for participative environments.

2.1. Direct Component

The direct component, $E_{d_\lambda}(x)$, is defined as

$$E_{d_\lambda}(x) = J_\lambda(x) e^{-cd(x)}, \quad (2)$$

where $J_\lambda(x)$ is the signal with no degradation, which is attenuated by $e^{-cd(x)}$, named as transmission $t(x)$. We propose that, considering $J_\lambda(x)$ as a general image taken from a Lambertian Surface, $J_\lambda(x)$ can also be described by the color constancy image formation model [26]

$$J_\lambda(x) = L_\lambda(x) M_\lambda(x) C_\lambda(x), \quad (3)$$

where $L_\lambda(x)$ is the light source, $M_\lambda(x)$ is the reflectivity of the imaged object, and $C_\lambda(x)$ are the camera parameters. Omitting the camera parameters and considering the light source as constant, we have that

$$J_\lambda(x) = L_\lambda M_\lambda(x). \quad (4)$$

In participative environment images, the natural light comes from a limited cone above the scene, as portrayed in Fig. 1 as ROI_o optical manhole cone [5]. For this reason, we assume that the light source is related to the cone size and also influenced by the environment.

2.2. Backscattering Component

Following the Jaffe-McGlamery [15] and [19], and the respective simplifications [22] and [4], the backscattering component, $E_{bs_\lambda}(x)$, can be defined as

$$E_{bs_\lambda}(x) = A_\lambda^D \cdot (1 - t(x)), \quad (5)$$

where A_λ^D is the veiling light, here also called ambient light constant, that represents the color and radiance characteristics of the media. This constant is related to the ROI_p , analogous to ROI_o , placed above the LOS (Line of Sight). Also, this constant is altered by the depth and influenced by the environment. The $(1 - t(x))$ portion weights the effect of the backscattering as a function of the distance, $d(x)$, from the object to the camera. The higher the distance, the higher the chance that A_λ^D scatters over the scene.

2.3. Final Model

By considering low depth variations in the same captured scene we can consider that the LOS and the objects are all illuminated by the same light source. The main consideration of this section is that the ambient light, A_λ^D , and the constant light source, L_λ , are actually the same. Thus, by considering $L_\lambda = A_\lambda^D$ in Eqs. (2) and (4) the final equation is defined as

$$I_\lambda(x) = A_\lambda^D \cdot M(x) \cdot t(x) + A_\lambda^D \cdot (1 - t(x)). \quad (6)$$

Note that this equation presents a generalization from the *Koschmieder's* equation [16] that is commonly used by de-hazing methods, *e.g.* [13] and [8]. When $A_\lambda^D \approx [1, 1, 1]$ (approximately white) Eq. (6) turns into the *Koschmieder's* equation. We show in Section 6 that, by using Eq. (6) in restoration, we can jointly obtain color recovering and haze removal by solving a single equation.

3. Related Works

In order to estimate the true object color reflectivity, both the transmission and the ambient light must be estimated.

Toward that end, one has to assume some properties a haze-free image should have, *i.e.*, an image without ambient interference. These properties are usually image priors, or assumptions that can be used to find *indicators* of the amount of turbidity a certain image patch has.

Fattal [8] has assumed that there is no covariance between the reflectance and the illumination, so that the transmission can be defined as the source of covariance. However, it has been shown that the assumption works only for low degradation conditions [9].

Fattal also proposed a method to estimate the transmission that uses a *color line assumption* [20]. It infers the transmission by finding the intersection point between the color line and the vector with the orientation of the veiling light. A robust method is obtained. However, it depends on finding patches where some model properties exist.

One of the main methods developed is based on the Dark Channel Prior [13], where the minimum value of the image channels in a patch gives an indication of the transmission, $t(x)$. This is a robust idea, but it is developed solely for white colored haze and does not work well for underwater environments [6]. The same method has been adapted several times for underwater environments, *e.g.* [3], [4], [11], and [18]. However, all adaptations lacked to consider the large range of colors that exist underwater by assuming some specific conditions such as the Red Channel Absorption [11]. Our modeling (Section 2) do not consider the participative media as having single color properties. We show later that this consideration is helpful in achieving accurate image restoration from any type of environment.

There are also approaches that directly manipulate some of the image properties, *e.g.* contrast, blur, and noise, in order to try to improve them. Many general image enhancing methods can be used to recover the visibility through turbid media, *e.g.* CLAHE [14], Bilateral Filters [25], and Color Constancy. There are examples of enhancement method fusions in the literature, *e.g.* [1] and [2]. The direct manipulation of the image properties reduces the haze at the cost of also degrading some of the image properties. Moreover, enhancement methods do not usually consider the spatial variation that exists in participative media degraded images.

4. Composite Prior Transmission Estimation

The use of a single indicator, such as the color [4] and [13], or the contrast [24], is *decisive* but not *sufficient*. For instance, it is not possible to know if a signal corresponds to an object reflectance of a given color, or if it has a certain color due to the ambient light. The same happens to the image structure, *i.e.* it is not possible to know if a patch has a certain weak structure or if this structure is already attenuated by the turbidity.

In contrast, we believe that, when a pixel has a high transmission, this indication is usually related to the infor-

mation of the signal, and unrelated to the veiling. Thus, we propose a simple combination of transmission estimators using the maximum between each of them. This combination is constrained by using indicators that output over distinct types of patches.

In this work we propose the *Composite Transmission* by joining two transmission indicators. We denote the transmission of a pixel x as being

$$t(x) = \max(t_v(x), t_c(x)), \quad (7)$$

where $t_v(x)$ is the transmission computed with a color-based *Veil Difference Transmission* and $t_c(x)$ is the transmission computed with the *Contrast Transmission*.¹

4.1. Veil Difference Transmission

Considering the ambient light, we propose the following assumption: the image tends to be closer to the ambient light when the image is affected by turbidity. Fig. 2 shows the histogram of a single scene that is captured under different turbidity levels (Fig. 8). It can be seen that the intensities of the pixels tend to be closer to the ambient light (represented by dashed lines) as the amount of turbidity increases.

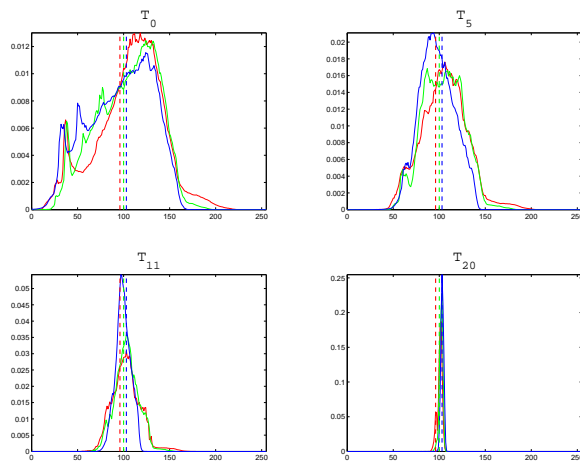


Figure 2: Histograms of the same scene captured under different levels of turbidity. T0 is an image free of turbidity. T5, T11 and T20 have different turbidity levels created through the addition of milk [7]. Fig. 8 shows the images used.

Given that we assume all pixels from a patch $\Omega(x)$, centered at x , to have the same distance to the camera, we define the transmission as

$$t_v(x) = \frac{\max_{\lambda \in \{r,g,b\}} \max_{y \in \Omega(x)} (|I_\lambda(y) - A_\lambda^D|)}{\max_{\lambda \in \{r,g,b\}} \max_{y \in \Omega(x)} (|J_\lambda(y) - A_\lambda^D|)}, \quad (8)$$

¹To compute the transmission, we assume A_λ^D as given.

where the transmission, $t_v(x)$, can be interpreted as the loss of distinction to A_λ^D between the haze-free image, J_λ , and the turbid image I_λ . We take pixel of the channel with the highest difference since it is the one with more information. The problem is that the haze-free image is unknown. However, when looking at haze-free images, we perceive that they tend to have a significantly difference to the light source on at least one of its color channels. Formally, for an image J_λ , we define the Veil Difference Prior as

$$\max_{\lambda \in \{r,g,b\}} (\max_{y \in \Omega(x)} (|J_\lambda(y) - A_\lambda^D|)) = \max_{\lambda \in \{r,g,b\}} (\max(1 - A_\lambda^D, A_\lambda^D)). \quad (9)$$

This prior can be further understood as a *generalization* of the dark channel prior from *He et al.* [13]. Considering the ambient light color as pure white, *i.e.* $A_\lambda^D = [1, 1, 1]$, Eq. (9) turns into $\max(1 - J_\lambda(x)) = 1$ for $\lambda \in \{r, g, b\}$, which is analogous to the dark channel prior. By replacing Eq. (9) into Eq. (8) we define the veil difference transmission computed as

$$t_v(x) = \frac{\max_{\lambda \in \{r,g,b\}} (\max_{y \in \Omega(x)} (|I_\lambda(y) - A_\lambda^D|))}{\max_{\lambda \in \{r,g,b\}} (\max(1 - A_\lambda^D, A_\lambda^D))}. \quad (10)$$

We show the resultant veil difference transmission on Fig. 5b. We can perceive that this transmission captures the distance variation existent on the image.

4.2. Contrast Transmission

We can observe on Fig. 2 that, besides the color approximation to veiling light, we have shrinking into the histogram shape, dramatically reducing the global image contrast. Thus, we assume the following local indicator: for a given patch I_λ , the contrast of this patch tends to reduce proportionally to an increase at the turbidity.

We selected a contrast function that is a *valid* indicator, with this, we define the contrast transmission

$$t_c(x) = \frac{\max_{\lambda \in \{r,g,b\}} (\max_{y \in \Omega(x)} (I_\lambda(y)) - \min(I_\lambda(y)))}{\max_{\lambda \in \{r,g,b\}} (\max_{y \in \Omega(x)} (J_\lambda(y)) - \min(J_\lambda(y)))}, \quad (11)$$

this ratio, analogously to Eq. (8), represents the lost of contrast information caused by the turbidity. However, we do not know the contrast of the haze free version of image. So, we assume that this haze free image patch has the maximum possible range defining the Contrast Prior as

$$\max_{\lambda \in \{r,g,b\}} (\max_{y \in \Omega(x)} (J_\lambda(y)) - \min(J_\lambda(y))) = 1. \quad (12)$$

This is true for some samples of the image. Since we are not using only this indicator, it is reasonable to make this assumption. Thus, we have the contrast transmission computed as

$$t_c(x) = \max_{\lambda \in \{r,g,b\}} (\max_{y \in \Omega(x)} (I_\lambda(y)) - \min(I_\lambda(y))). \quad (13)$$

We show the resultant contrast transmission on Fig. 5c. We can perceive that this transmission is sparse, but has a clear representation of the distance variation.

We also show the contribution from each of the image priors after applying Eq. (7) on Fig. 5d. We perceive that the intermediate range transmissions are dominated by the contrast transmission.²

4.3. Priors Validation

To evaluate the proposed priors, we compute the average histogram for different priors on 2,000 images for a haze-free and a participative media dataset. The images were resized into a maximum side of 1,024 and the priors were computed over patches of 15x15 pixels.

For haze-free dataset we used images from the test set of the popular ImageNet [21]. For participative media, we built a dataset by collecting turbid images over the web. Some samples of these participative media images are shown on Fig. 3. The dataset was made to be diverse and contain samples of several kinds of media, *e.g.*, fog, oceanic water, coastal water, sand storm etc.

On these datasets we test the Veil Difference Prior (*VDP*) (Eq. (9)) and the *Composite Prior* (*CP*) that takes the maximum between Eq. 10 and Eq. (13). We also compare the histograms with the Dark Channel Prior (*DCP*) [13], and the *UDCP* prior [6].



Figure 3: The participative media dataset used to test the priors on a more general setting of turbid places. We collected around 2,000 images over the web containing all kinds of participative media.

Fig. 4 shows the generated histograms. We can confirm that the *DCP* of the images is approximately one (Fig. 4a), however, it tends to have a similar behaviour for participative media images, which demonstrates non-sensibility to general participative media. The same, in a lesser extent, happens for the *UDCP* prior (Figs. 4c and 4d).

²Please refer to the supplementary material for further comparisons on the transmission estimations.

For the *VDP* (Figs. 4e and 4f), it showed around 40% of the bins equal to one and a tendency to have higher values. This result shows that the prior is clearly not as strong as the *DCP*. However, the average for the prior on degraded participative media showed a very high range of values, indicating a sensitivity to the presence of turbidity.

Finally, we show the histograms for the Composite Prior, arguably to be the most reliable behaviour. For haze-free images (Fig. 4g) there is a clearer tendency of assuming the value one than just the veil difference prior. Yet, it showed less range of results on participative media images (Fig. 4h), mainly due to the tendency on still finding structures. However, it combines the best of two worlds, having high range of values for participative media images, and a solid high response for haze-free images. This corroborates about the generality of the proposed priors.

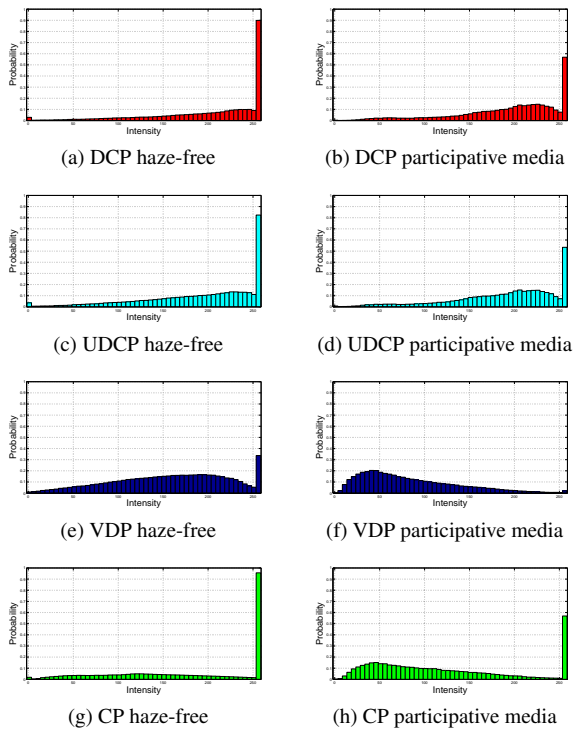


Figure 4: The histograms computed for, on the left, haze free images (Image Net), on the right, general participative media images (Fig. 3). For a better understanding of results, we show sampling of the histograms on every five bins. For an easier comparison we plotted $1 - DCP$ and also $1 - UDCP$.

4.4. Refining Transmission

When the transmission is computed over a patch, there may be considerable intensity variations that do not agree with a single transmission. For that, the transmission map

$t(x)$ must be refined. We choose to use the soft matting algorithm on $t(x)$ [17]. The mentioned algorithm can be applied since there is some relation between the Eq. (6) and the definition of the matting problem given by the equation:

$$I = F\alpha + B(1 - \alpha), \quad (14)$$

Thus, α for the matting problem is the same as the transmission for the haze removal problem. The results of a refined transmission are shown on Fig. 5e.

5. Image Restoration

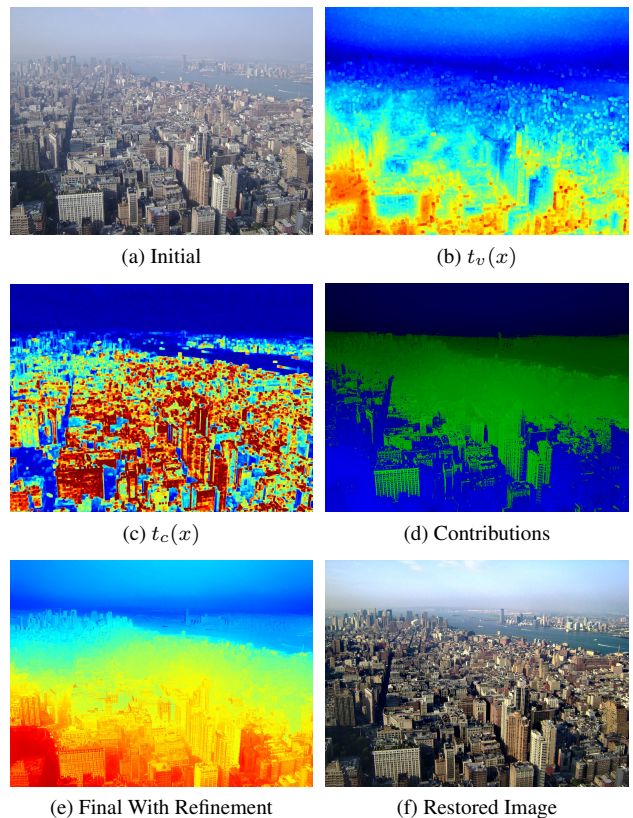


Figure 5: The results from the proposed method and the transmission maps. (a) The input fog image. (b) veil difference transmission $t_v(x)$. (c) Contrast transmission $t_c(x)$. (d) The contribution of each transmission after the max operator, where green is $t_c(x)$ and blue is $t_v(x)$. (e) The image after the refinement with the soft matting algorithm. (f) The restored image.

In this section, first we show the estimation of the ambient light constant A_λ^D . Then we also show a way to reduce image noise and, finally, the restoration process that uses our novel model derivation from Sec. 2.

5.1. Estimating the Ambient Light

The ambient or veiling light is associated with the light color and intensity that is scattered to the scene, and as stated on Sec. 2. As stated by [23], a correct estimation of the ambient light is fundamental, since all the calculated transmission uses it as reference. Initially, many authors estimated it as being the brightest pixels in the image [24] [8]. This estimation presents some downsides, specially if the ambient light is not present on the image. *Sulami et al.* proposed a method [23], that divides the estimation into orientation and magnitude and do not need the presence of an ambient light pixel on the image, however it depends on finding patches that obeys certain properties.

As we stated on Section 2, the ambient light is associated with the light source on the scene. With this, it is reasonable to use color constancy techniques, commonly used to find the light source color on general images. Techniques such as gray edge [26], the gray world, the max-rgb or the shades-of-gray [10] can be used. The problem with gray edge is that the edges are normally blurry and the gray world technique fails when there are too many close objects. Also, max-rgb is dependent on actually having white patches fully reflecting the light information. Preliminary tests shows that using the shades-of-gray algorithm encapsulates the best behaviour in our case. The algorithm does so by doing an estimation in between the average of the scene and the reflectivity of a white patch.

5.2. Ensuring Model Integrity

As we discussed previously, the images captured in participative media are intensively affected by the backscattering effect. Besides that, the process of photometry in participative media is very prone to noise and blur. In order to effectively estimate the transmission related to the effects of backscattering it is necessary to minimize other effects that may occur.

The bilateral filter [25] is the function we choose to improve the results. It tends to eliminate the high frequency isolated points but keeps the edges, where it is likely to have greater variation of transmission. This reduces the blurring effect and the noise conditions but keep the backscattering for estimation. With this, we choose to apply this function before computing the veil difference transmission.

5.3. Restoration

The image with restored visibility (see Fig. 5f) is obtained by isolating the object reflectivity $M(x)$ on equation 6:

$$M_\lambda(x) = \frac{I_\lambda(x) - A_\lambda^D + A_\lambda^D t(x)}{\max(t_{\lambda 0}, A_\lambda^D t(x))}, \quad (15)$$

where the $t_{\lambda 0}$ parameter is the minimum transmission. This parameter is useful when there are no information behind

the veil, avoiding to restore noise. Here we use three minimum parameters, t_{r0} , t_{g0} and t_{b0} , where, normally, setting them between 0.1 and 0.2. However, for some images, where for instance, there is low red channel information, it is reasonable to set t_{r0} higher to avoid saturation.

6. Evaluation

All our results were obtained by C++ implementations using OpenCV for matrices manipulation. All the parameters are kept as explained on Section 5. We first compare the results by directly comparing them visually with previous state-of-the-art results. For most of the cases, we used the provided images by the authors in order to reproduce the results. To produce the Red Channel [11] and He [13] transmissions, we made a C++ implementation. For all UDCP [6] results, we used an implementation provided by the authors.

6.1. Qualitative Evaluation

Fig. 6 shows the results obtained for the underwater environment. First of all, when comparing the transmission maps (Fig. 6 first and third row), the proposed method tends to not overestimate transmission. This happens mainly due to the observation that the ambient light color is not necessarily present on the image. Further, we perceive that the use of a transmission that also contains structure, helps on not underestimating the transmission on structured regions. The Red Channel assumption works quite well for Fig. 6 with a little overestimation. However, for the scuba-divers image (Fig. 6i), this method clearly has problems by overestimating highly red objects but with high amount of degradation.

Also, when comparing the results with [1] (Figs. 6e and 6m) there is a clear tendency of our method to have more contrasted colors and less noise, but with slightly less contrast.

We proposed a model that consider color variation on participative media. With this idea, our method is capable of recovering color properties without further use of white balances and compensations. This can be seen when comparing the proposed method with *Drews et al.* [13] [6], where a good restoration was obtained (Fig 6f) but with a not satisfactory color correction.

As stated earlier, our method is designed to restore any kind of participative media without any parameter adjustment. On Fig. 7 we show the results comparing with other state-of-the-art methods. Once more, the fact that we suppose that the ambient light is not a pixel from the scene helps not to overestimate transmission on lower distances, where we obtain a much clearer result. However, for the same reason, on longer distances, our method culminates into overestimating the transmission. Finally, we also see a better color correction when compared to *Fattal* [9] and

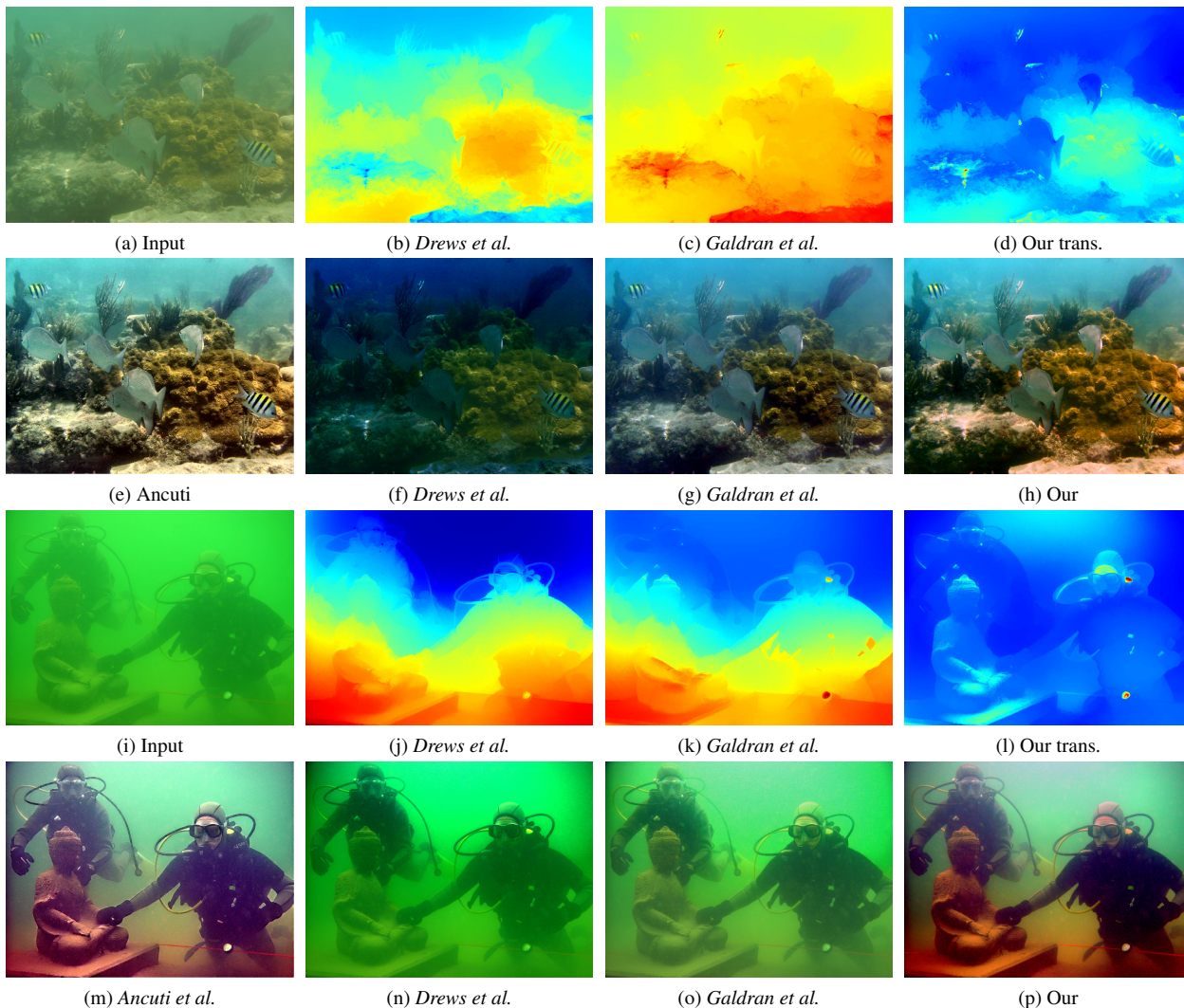


Figure 6: Results showing the transmission estimation and restoration for underwater images. The transmissions are shown using a red to blue scale, where red indicates a higher transmission. The obtained results are compared with *Galdran et al.* [11], *Drews et al.* [6] and *Ancuti et al.* [1].

He et al. [13]. We explain this color enhancement due to the fact that we do not consider fog as being approximately white.

6.2. Quantitative Evaluation

Usually methods are compared subjectively by the perception of image quality. However in many cases, such as when comparing Figs. 6e and 6h, it is hard to access which of the methods obtained the best haze removal.

An effective way to access dehazing algorithms quality is by comparing them with a ground truth, a version of the same image without turbidity. For this, we used the TURBID dataset proposed on [7]. They reproduced a scene of an underwater environment where multiple images are captured with an increasing turbidity by addition of milk. Fig.

8 shows four image samples of the TURBID dataset.

We plot on Fig. 9 the mean square error in function of turbidity (proportional to the amount of milk). The error is measured between the restored image and the clean image (no milk). We compare our result with the Red Channel Prior (RCP) [11], the Dark Channel Prior (DCP) [13] and also the TURBID images. On the TURBID images (Blue Line) we compare the mean square error of the turbid images without any kind of restoration. The other lines show the error after the restoration. Considering this, when error is below the TURBID images lines, it shows that the method performed an effective restoration. This is true since the image became closer to the reference image.

On Fig. 9a, we measured the results of each method by setting a fixed ambient light estimation. We can perceive

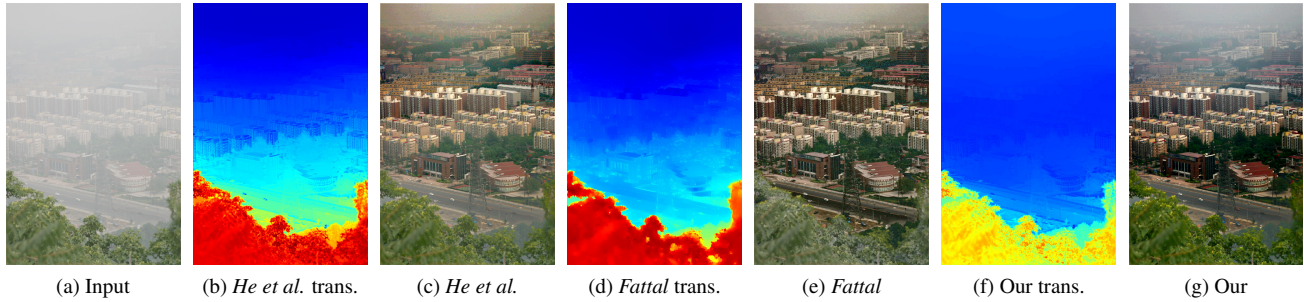


Figure 7: Results for a fog image dehazing. We compare the proposed method with some state-of-the-art methods, *Fattal* [9] and *He et al.* [13].

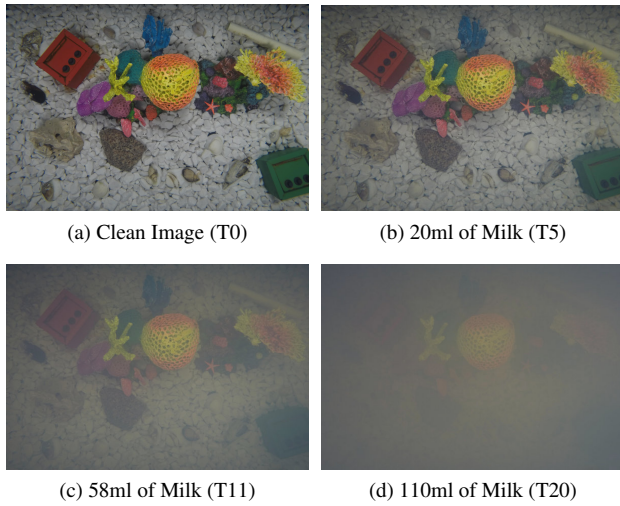


Figure 8: Some samples of the TURBID dataset [7] used to evaluate the quality of image restoration.

that the proposed method got the lowest average error, just having a higher error than DCP on very turbid images.

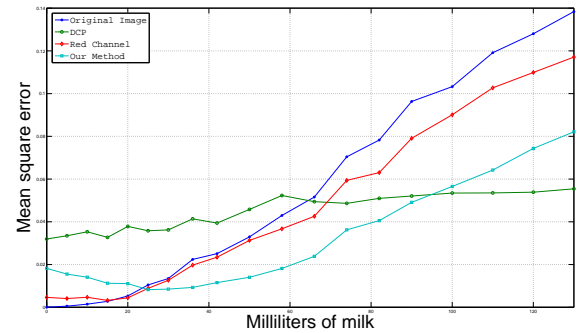
On Fig. 9b, we measured the results of each method by using the own ambient light estimation of the method. The proposed method was considerably better, since the ambient light estimation for this dataset not accurate for the DCP or the RCP considering it is not present on the image.³

7. Conclusions

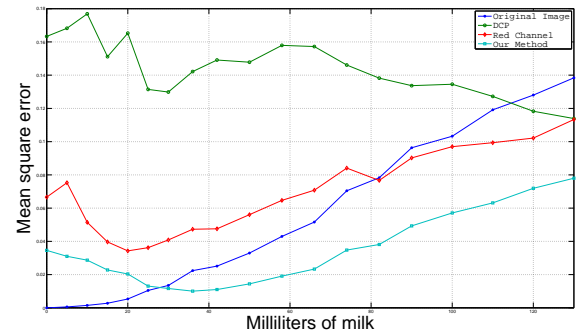
In this paper we proposed a novel automatic image restoration method to restore images captured in participative media.

We contributed to the theoretical modeling by proposing a new simplification to the image formation model that considers color changes in the participative media. We also proposed a new way to estimate image transmission by jointly using different novel image priors. These priors were veri-

³To get all the restored images, refer to the supplementary material.



(a) A_{λ}^D fixed



(b) A_{λ}^D estimated

Figure 9: Objective evaluation of the proposed method using the TURBID dataset. The curves represents the MSE in function of turbidity (Simulated by Milk). Each turbid image is compared with the clear image (Fig. 8a).

fied using different datasets.

This image transmission was refined by soft matting and better estimated by ensuring the model integrity with the bilateral filter. We proposed that the ambient light, or veiling light can be successfully estimated by using color constancy techniques, specially the shades-of-gray [10]. All of this contributions led into a restoration method capable

of restoring colors independent of the type of participative media used.

We tested the proposed method with different kinds of participative media obtaining state-of-the-art results on most of them. Finally, we also tested the method objectively by using the TURBID dataset [7] to be able to compare restored images with a ground truth.

As a future work, we would like to study the behaviours of the fusion with other transmission estimators.

References

- [1] C. Ancuti, C. O. Ancuti, T. Haber, and P. Bekaert. Enhancing underwater images and videos by fusion. In *Computer Vision and Pattern Recognition (CVPR), 2012 IEEE Conference on*, pages 81–88. IEEE, 2012.
- [2] S. Bazeille, I. Quidu, L. Jaulin, and J.-P. Malkasse. Automatic underwater image pre-processing. In *CMM'06*, page xx, 2006.
- [3] N. Carlevaris-Bianco, A. Mohan, and R. M. Eustice. Initial results in underwater single image dehazing. In *OCEANS 2010*, pages 1–8. IEEE, 2010.
- [4] J. Y. Chiang and Y.-C. Chen. Underwater image enhancement by wavelength compensation and dehazing. *Image Processing, IEEE Transactions on*, 21(4):1756–1769, 2012.
- [5] T. W. Cronin and N. Shashar. The linearly polarized light field in clear, tropical marine waters: spatial and temporal variation of light intensity, degree of polarization and e-vector angle. *Journal of Experimental Biology*, 204(14):2461–2467, 2001.
- [6] P. Drews, E. do Nascimento, F. Moraes, S. Botelho, and M. Campos. Transmission estimation in underwater single images. In *Computer Vision Workshops (ICCVW), 2013 IEEE International Conference on*, pages 825–830. IEEE, 2013.
- [7] N. D. S. B. F. Codevilla, J. Gaya. Achieving turbidity robustness on underwater images local feature detection. *BMVC 2015*, 26:157, 2015.
- [8] R. Fattal. Single image dehazing. In *ACM Transactions on Graphics (TOG)*, volume 27, page 72. ACM, 2008.
- [9] R. Fattal. Dehazing using color-lines. *ACM Transactions on Graphics (TOG)*, 34(1):13, 2014.
- [10] G. D. Finlayson and E. Trezzi. Shades of gray and colour constancy. In *Color Imaging Conference*, pages 37–41, 2004.
- [11] A. Galdran, D. Pardo, A. Picón, and A. Alvarez-Gila. Automatic red-channel underwater image restoration. *Journal of Visual Communication and Image Representation*, 26:132–145, 2015.
- [12] D.-M. He and G. G. Seet. Underwater lidar imaging in highly turbid waters. In *International Symposium on Optical Science and Technology*, pages 71–81. International Society for Optics and Photonics, 2002.
- [13] K. He, J. Sun, and X. Tang. Single image haze removal using dark channel prior. *Pattern Analysis and Machine Intelligence, IEEE Transactions on*, 33(12):2341–2353, 2011.
- [14] R. Hummel. Image enhancement by histogram transformation. *Computer graphics and image processing*, 6(2):184–195, 1977.
- [15] J. S. Jaffe. Computer modeling and the design of optimal underwater imaging systems. *Oceanic Engineering, IEEE Journal of*, 15(2):101–111, 1990.
- [16] H. Koschmeider. Theorie der horizontalen sichtweite. *Beitr. Phys. Freien Atm.*, pages 12:171–181, 1990.
- [17] A. Levin, D. Lischinski, and Y. Weiss. A closed-form solution to natural image matting. *Pattern Analysis and Machine Intelligence, IEEE Transactions on*, 30(2):228–242, 2008.
- [18] H. Lu, Y. Li, L. Zhang, and S. Serikawa. Contrast enhancement for images in turbid water. *JOSA A*, 32(5):886–893, 2015.
- [19] B. McGlamery. A computer model for underwater camera systems. In *Ocean Optics VI*, pages 221–231. International Society for Optics and Photonics, 1980.
- [20] I. Omer and M. Werman. Color lines: Image specific color representation. In *Computer Vision and Pattern Recognition, 2004. CVPR 2004. Proceedings of the 2004 IEEE Computer Society Conference on*, volume 2, pages II–946. IEEE.
- [21] O. Russakovsky, J. Deng, H. Su, J. Krause, S. Satheesh, S. Ma, Z. Huang, A. Karpathy, A. Khosla, M. Bernstein, A. C. Berg, and L. Fei-Fei. ImageNet Large Scale Visual Recognition Challenge. *International Journal of Computer Vision (IJCV)*, pages 1–42, April 2015.
- [22] Y. Schechner and N. Karpel. Recovery of underwater visibility and structure by polarization analysis. *Oceanic Engineering, IEEE Journal of*, 30(3):570–587, July 2005.
- [23] M. Sulami, I. Geltzer, R. Fattal, and M. Werman. Automatic recovery of the atmospheric light in hazy images. In *IEEE International Conference on Computational Photography (ICCP)*, 2014.
- [24] R. T. Tan. Visibility in bad weather from a single image. In *Computer Vision and Pattern Recognition, 2008. CVPR 2008. IEEE Conference on*, pages 1–8. IEEE, 2008.
- [25] C. Tomasi and R. Manduchi. Bilateral filtering for gray and color images. In *Computer Vision, 1998. Sixth International Conference on*, pages 839–846. IEEE, 1998.
- [26] J. Van De Weijer, T. Gevers, and A. Gijsenij. Edge-based color constancy. *Image Processing, IEEE Transactions on*, 16(9):2207–2214, 2007.